

SUPPLEMENTAL MATERIAL

Liu et al., <http://www.jem.org/cgi/content/full/jem.20110958/DC1>

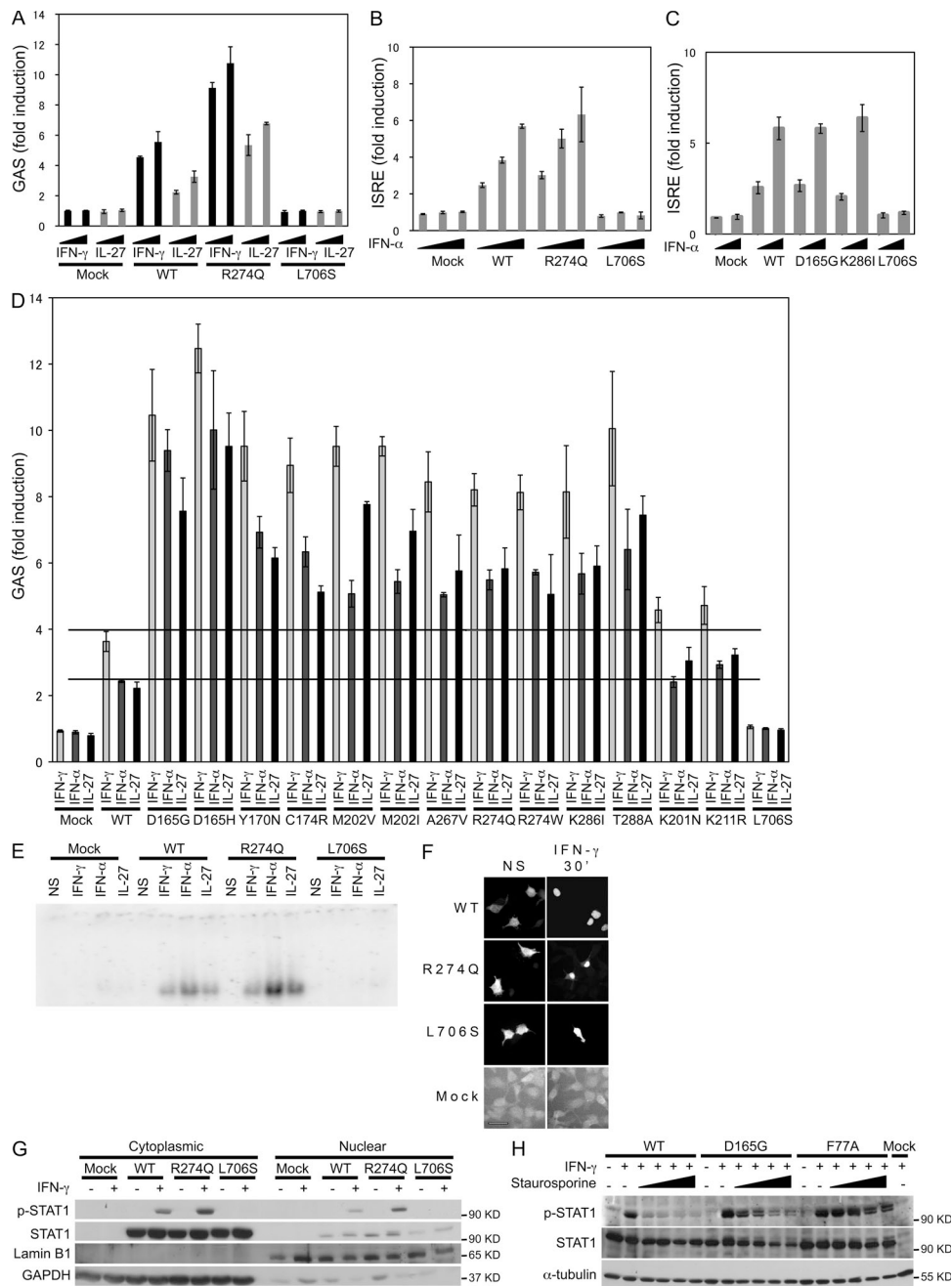


Figure S1. STAT1-CMCD mutants are gain-of-function alleles by loss of nuclear dephosphorylation. The response to various doses of IFN- γ , IFN- α or IL-27 (A-C) was evaluated by determining luciferase activity of reporter genes under the control of the GAS promoter (A) and the ISRE promoter (B and C), in U3C cells transfected with a mock vector, a WT form, or the mutant forms (R274Q, D165G, K286I and L706S) of *STAT1*. Experiments were performed independently at least three times. (D) The response to IFN- γ , IFN- α , and IL-27 was evaluated by determining luciferase activity of a reporter gene under the control of the GAS promoter in U3C cells transfected with a mock vector, a WT allele of *STAT1*, or 11 CMCD-causing *STAT1* alleles (D165G, D165H, Y170N, C174R, M202V, M202I, A267V, R274Q, R274W, K286I, and T288A), as well as the known K201N, K211R, and L706S *STAT1* alleles. The two horizontal lanes show the response of the WT *STAT1* allele to cytokine stimulation. The experiment was performed twice. (E) GAF-DNA-binding activity in U3C cells transfected with mock, WT, R274Q, and L706S alleles of *STAT1*; left unstimulated (NS); or stimulated with IFN- γ , IFN- α , or IL-27; the results shown are representative of at least two independent experiments. (F) Immunofluorescence of U3C cells transfected with WT, R274Q, and L706S alleles of *STAT1* without (NS) and with IFN- γ stimulation and stained with an antibody specific for *STAT1*. Bar, 50 μ m. The pictures shown are representative of the cells observed. (G) The cytoplasmic (visualized by the GAPDH antibody) and nuclear (visualized by the Lamin B1 antibody) fractions of U3C cells transfected with mock, WT, R274Q, and L706S alleles of *STAT1*, with and without IFN- γ stimulation, were tested for the presence of total and phosphorylated *STAT1* by WB. We loaded the equivalent of 25 μ g of protein for the cytoplasmic fraction and 8 μ g of protein for the nuclear fraction. The experiment was performed twice. (H) The nuclear dephosphorylation of *STAT1* was assessed in U3C cells transfected with a mock vector, a WT *STAT1* allele, the D165G, and the F77A *STAT1* mutant alleles (the latter being known to impair *STAT1* dephosphorylation) after treatment with IFN- γ and the tyrosine kinase inhibitor staurosporine for increasing periods of time (30, 60, 90, and 120 min); the results shown are representative of at least two independent experiments.

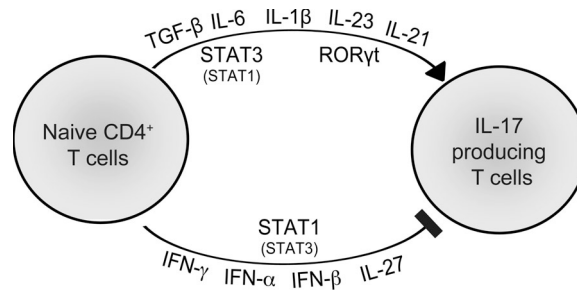


Figure S2. Schematic representation of the cytokines and transcription factors directing the development of naive CD4 T cells into IL-17-producing T cells. Activating molecules, such as IL-6, IL-1 β , IL-23, and IL-21 (acting mostly through STAT3, ROR γ t, and, to a lesser extent, STAT1), TGF- β , and inhibiting molecules, such as IFN- γ , IFN- β , IFN- α , and IL-27 (acting mostly through STAT1 and, to a lesser extent, STAT3) are represented.

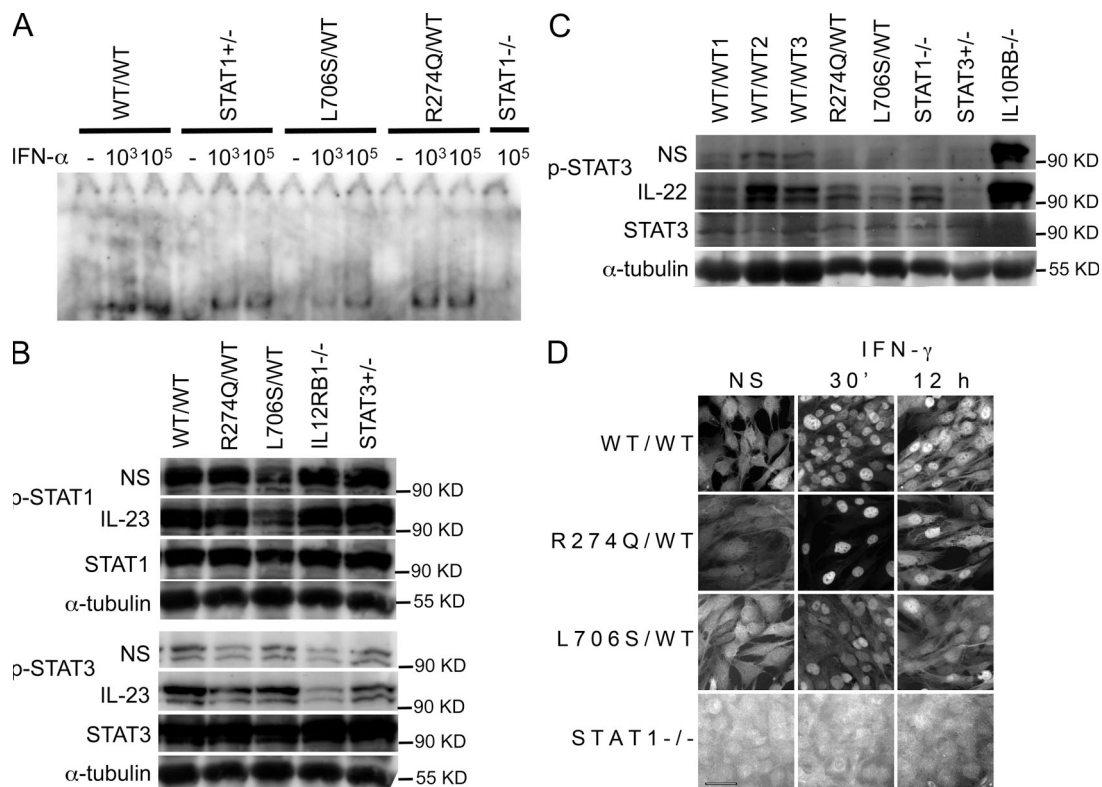


Figure S3. Normal response of CMCD patient cells to IFN- α in terms of ISGF3 activation; to IFN- γ in terms of STA1 nuclear translocation; and to IL-23 and IL-22 in terms of pSTAT3. (A) The response of the (R274Q/WT) patient's EBV-B cells was evaluated by EMSA with an ISRE probe and was compared to those of a healthy control (WT/WT), heterozygous cells with a WT and a loss-of-function allele (STAT1^{+/-}), cells heterozygous for a dominant loss-of-function mutation of *STAT1* (L706S/WT), and cells with complete *STAT1* deficiency (STAT1^{-/-}). Cells were stimulated with various doses of IFN- α (international unit/milliliter); the results shown are representative of at least two independent experiments. (B) The response to IL-23 of T cell blasts was evaluated in control (WT/WT), CMCD (R274Q/WT), MSMD (L706S/WT), IL12RB1-deficient (IL12RB1^{-/-}) and heterozygous *STAT3* (STAT3^{+/-}) cells by WB. The experiment was performed twice. (C) The response to IL-22 of primary fibroblasts was evaluated in three controls (WT/WT1, 2, and 3), CMCD (R274Q/WT), MSMD (L706S/WT), *STAT1*-deficient (STAT1^{-/-}), heterozygous *STAT3* (STAT3^{+/-}), and IL10RB-deficient (IL10RB^{-/-}) cells by WB; the results shown are representative of at least two independent experiments. (D) Immunofluorescence for STAT1 of SV-40-transformed fibroblasts with and without IFN- γ stimulation, for a control (WT/WT), a CMCD patient (R274Q/WT), an MSMD patient (L706S/WT), and a complete *STAT1*-deficient patient (STAT1^{-/-}). Bar, 50 μ m. The results shown are representative of at least two independent experiments

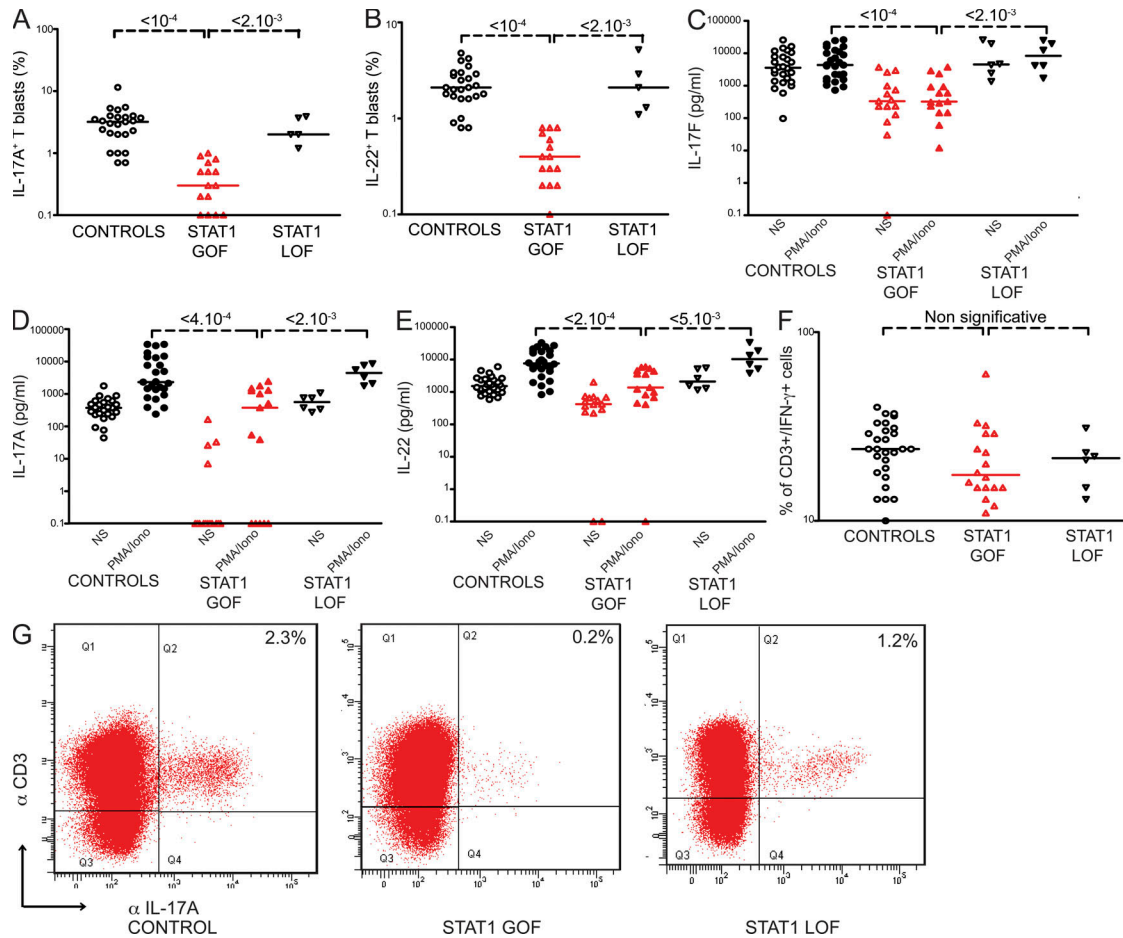


Figure S4. Impaired in vitro differentiation of IL-17- and IL-22-producing T cells in patients with AD CMCD and *STAT1* mutations. Each symbol represents an individual control (black circles), a patient with a *STAT1* GOF mutation (red triangles), or a patient with one or two *STAT1* LOF mutations (black upside-down triangles). The results shown are representative of at least two independent experiments. (A and B) IL-17⁺ (A) and IL-22⁺ (B) T cell blasts were expanded in vitro in presence of anti-CD3 antibody, IL-2, IL-1β, and IL-6 for 5 d, followed by 12 h of stimulation with PMA and ionomycin. C- E. Secretion of IL-17F (C), IL-17A (D), and IL-22 (E) by T cell blasts expanded in vitro in presence of anti-CD3 antibody, IL-2, IL-1β, and IL-6 for 5 d, followed by 12 h of stimulation with PMA and ionomycin. Horizontal bars represent medians. The p-values for the nonparametric Wilcoxon test, between patients with *STAT1* GOF mutations ($n = 18$) and healthy controls ($n = 28$) and patients with *STAT1* LOF mutations ($n = 6$) are indicated. All differences between healthy controls and patients with *STAT1* LOF alleles were nonsignificant. (F) Percentage of CD3⁺/IFN-γ⁺ cells, as determined by flow cytometry, in nonadherent PBMCs activated by incubation for 12 h with PMA and ionomycin. Horizontal bars represent medians. The p-values for differences between patients with *STAT1* GOF mutations ($n = 18$) and healthy controls ($n = 28$) and patients with *STAT1* LOF mutations ($n = 6$) were calculated in nonparametric Wilcoxon tests and were nonsignificant. (G) Flow cytometry analysis of CD3 and IL-17A in nonadherent PBMCs activated with PMA-ionomycin, from a control (left), a *STAT1* GOF patient (middle), and a *STAT1* LOF patient (right). The percentage of CD3⁺/IL17A⁺ cells is indicated in the top right corner of each dot plot.

Table S1, which shows all novel coding heterozygous variants found by whole exome sequencing in six different patients, is available as an excel file.

Table S2, which shows all novel coding heterozygous variants found by whole-exome sequencing within genes shared by more than one patient, is available as an excel file.

Table S3. Conservation and predictions on the function of the mutant *STAT1* alleles associated with CMCD

Mutation	Polyphen II score	Damaging	Conservation
D165G	0.247	Possibly	Poor (E, N, Y found at this position)
D165H	0.469	Possibly	
Y170N	0.819	Possibly	Poor (R, H, F found at this position)
C174R	0.000	Benign	Very Poor (R found in two fishes, plus H, F, I, E Y, N, M, K)
M202V	0.794	Possibly	High (V found in the fish)
M202I	0.956	Probably	
A267V	0.998	Probably	High (G and I found at this position)
Q271P	0.932	Possibly	High (F and L found at this position)
R274W	1.000	Probably	Very High (no variation found at this position)
R274Q			
K286I	0.961	Probably	Very High (no variation found at this position)
T288A	0.997	Probably	High (S found at this position in the fish)

Summary of the Polyphen II score, possible functional consequences (possibly, probably damaging, or benign), and the conservation of the amino acid for the species sequenced for STAT1.

Table S4. Primers used for each STAT1 GOF mutation

Mutation	Primers (Forward+Reverse)
D165G	5'-AGA GCC TGG AAG GTT TAC AAG ATG A-3' 5'-TCA TCT TGT AAA CCT TCC AGG CTC T-3'
D165H	5'-AAG AGC CTG GAA CAT TTA CAA GAT G-3' 5'-CAT CTT GTAAAT GTT CCA GGC TCT T-3'
Y170N	5'-TTA CAA GAT GAA AAT GAC TTC AAA T-3' 5'-ATT TGA AGT CAT TTT CAT CTT GTAA-3'
C174R	5'-TAT GAC TTC AAA CGC AAA ACC TTG C-3' 5'-GCA AGG TTT TGC GTT TGA AGT CAT A-3'
M202I	5'-ACT CAA GAA GAT ATA TTT AAT GCT T-3' 5'-AAG CAT TAA ATA TAT CTT CTT GAG T-3'
M202V	5'-TTA CTC AAG AAG GTG TAT TTA ATG C-3' 5'-GCA TTA AAT ACA CCT TCT TGA GTAA-3'
A267V	5'-TCA CTA TAG TTG TGG AGA GTC TGC A-3' 5'-TGC AGA CTC TCC ACA ACT ATA GTG A-3'
R274Q	5'-TGC AGC AAG TTC AGC AGC AGC TTA A-3' 5'-TTA AGC TGC TGC TGA ACT TGC TGC A-3'
R274W	5'-CTG CAG CAA GTT TGG CAG CAG CTT A-3' 5'-TAA GCT GCT GCC AAA CTT GCT GCA G-3'
K286I	5'-AAT TGG AAC AGA TAT ACA CCT ACG A-3' 5'-TCG TAG GTG TAT ATC TGT TCC AAT T-3'
T288A	5'-GAA CAG AAA TAC GCC TAC GAA CAT G-3' 5'-CAT GTT CGT AGG CGT ATT TCT GTT C-3'
K211R	5'-ACA ATA AGA GAA GGG AAG TAG TTC A-3' 5'-TGA ACT ACT TCC CTT CTC TTA TTG T-3'